# Investigating the Efficiency of Drinking Water Treatment Sludge and Iron-Based Additives in Anaerobic Digestion of Dairy Manure: A Kinetic Modeling Study

## J. Rezaeifar[1], A. Rohani[1*], M. A. Ebrahimi-Nik[1]

1- Department of Biosystems Engineering, Faculty of Agriculture, Ferdowsi University of Mashhad, Mashhad, Iran
(*- Corresponding Author Email: arohani@um.ac.ir)

## Abstract

In the quest for enhanced anaerobic digestion (AD) performance and stability, iron-based additives as micro-nutrients and drinking water treatment sludge (DWTS) emerge as key players. This study investigates the kinetics of methane production during AD of dairy manure, incorporating varying concentrations of Fe and $Fe_3O_4$ (10, 20, and 30 mg $L^{-1}$) and DWTS (6, 12, and 18 mg $L^{-1}$). Leveraging an extensive library of non-linear regression (NLR) models, 26 candidates were scrutinized and eight emerged as robust predictors for the entire methane production process. The Michaelis-Menten model stood out as the superior choice, unraveling the kinetics of dairy manure AD with the specified additives. Fascinatingly, the findings revealed that different levels of DWTS showcased the highest methane production, while $Fe_3O_4$20 and $Fe_3O_4$30 recorded the lowest levels. Notably, DWTS6 demonstrated approximately 34% and 42% higher methane production compared to Fe20 and $Fe_3O_4$30, respectively, establishing it as the most effective treatment. Additionally, DWTS12 exhibited the highest rate of methane production, reaching an impressive 147.6 cc on the 6th day. Emphasizing the practical implications, this research underscores the applicability of the proposed model for analyzing other parameters and optimizing AD performance. By delving into the potential of iron-based additives and DWTS, this study opens doors to revolutionizing methane production from dairy manure and advancing sustainable waste management practices.

**Keywords**: Anaerobic digestion, Kinetic study, Livestock manure, Modeling, Trace elements

## Introduction

In recent decades, the world has witnessed an unprecedented surge in population and industrial development, especially in developing countries, leading to a remarkable rise in energy demand and waste generation. Improper waste management coupled with excessive reliance on conventional fossil fuels has contributed to environmental issues such as global warming and ozone layer depletion. Nonetheless, within the vast realm of biomass waste, lies a promising solution– the potential to tap into its renewable capacity and harness clean energy resources, like biofuels and biogas (Lu & Gao, 2021). The production of biogas from livestock manure has seen widespread adoption across numerous countries worldwide. In Iran, the Ministry of Agriculture reports a staggering population of over 8.4 million cattle and an annual beef production rate that has surged by 5%. Despite these statistics, except in a few industrial farms, a significant portion of the produced manure remains untreated and is often left in the open or directly applied to the land without composting. Nevertheless, Iran has immense potential for biogas production, with an

estimated yield of 16,146.35 million $m^3$ from various waste sources encompassing agricultural and animal wastes, and municipal and industrial wastewater. This abundance of potential biogas could produce substantial energy, totaling approximately 323 petajoules ($10^{15}$) and thus positioning Iran as a country with vast and valuable biogas resources (Zareei, 2018).

The process of anaerobic digestion (AD) stands as a remarkably efficient technique, facilitating the transformation of biomass waste into highly valuable end products. Foremost among these is biogas; predominantly composed of methane, carbon dioxide, and hydrogen (Wellinger, Murphy, & Baxter, 2013). Despite the rapid development of AD technology, some of its drawbacks such as low biodegradation efficiency, poor stability, and environmental sensitivity, have hindered its commercial application. To address these challenges, approaches such as co-digestion, pretreatment, and new reactor designs, as well as the use of additives have been proposed. The additives stimulate bacterial growth and reduce inhibitory effects which can help control microbial generation time, degradation rate, and gas production (Choong, Norli, Abdullah, & Yhaya, 2016; Gkotsis, Kougias, Mitrakas, & Zouboulis, 2023). Studies conducted by Al Seadi et al. (2008) and Cheng et al. (2020) emphasize the significance of incorporating trace elements or micro-nutrients like iron (Fe), cobalt (Co), or nickel (Ni) into the anaerobic digestion process. These additives play a crucial role in facilitating the digestion process.

Dudlet's research in 2019 reveals that iron has immense potential as a cost-effective enhancer in AD methane production. Furthermore, industrial enterprises generate around 18,895 thousand tonnes of iron waste every year, but only around 8,000 thousand tonnes get recycled and the remaining iron scraps are discarded into landfills (Dudley, 2019). Iron, being an essential element in the methanogenesis process, assumes a pivotal role in elevating biogas yield. Its unique capacity to ionize $Fe2+$ and $Fe3+$ ions enables it to serve as both an electron donor and acceptor. Chen, Konishi, & Nomura (2018) report that iron-based additives offer numerous advantages, including nutrient supplementation, improved methane yield, enhanced substrate digestibility, and effective control of $H_2S$ toxicity, among other benefits. A range of iron-based additives have common usage including waste iron scraps (Wiss), iron nanoparticles (Fe NPs), iron chlorides ($FeCl_2$, $FeCl_3$), zero valent scrap iron (ZVSI), iron oxides ($Fe_2O_3$, $Fe_3O_4$), iron powder (Fe powder), zero-valent iron (ZVI), iron sulfate ($FeSO_4$), and nano zero-valent iron (NZVI). Notably, waste iron scraps, iron oxides ($Fe_3O_4$), and iron powder emerge as prevalent and cost-effective additives due to the abundance of their sources and straightforward preparation methods. Additionally, these additives are commercially produced and readily available (Muddasar, 2022). Numerous studies have demonstrated the potential of these three types of iron-based additives to boost biogas yield and enhance process stability when utilized with diverse substrates. For instance, Cheng et al. (2020) observed a remarkable 64.4% increase in methane yield when rusted iron shavings were added to a mixture of food waste and municipal sludge. Furthermore, the addition of Fe powder led to a 14.46% rise in methane yield, while clean Fe scrap further elevated methane yield by 21.28% (Zhang, Feng, Yu, & Quan, 2014). Hao, Wei, Van, & Cao (2017) and Kong et al. (2018) have reported significant findings on the impact of adding Fe to anaerobic digesters handling the organic fraction of municipal solid waste (OFMSW) and sludge. The inclusion of Fe led to about 40% increase in $CH_4$ yield for OFMSW digestion and a 20% increase in sludge digestion. According to Abdelsalam et al. (2016), incorporating 20 mg/L Fe nanoparticles resulted in a 1.7-fold increase in biogas yield. Similarly, Ali, Mahar, Soomro, & Sherazi (2017) found that, when utilizing municipal solid waste (MSW) as a substrate for the AD process, the addition of 75 mg $L^{-1}$ concentration of $Fe_3O_4$ nanoparticles can lead to 72.09% enhancement

in methane generation. In another study by Noonari, Mahar, Sahito, & Brohi (2019), it was demonstrated that the introduction of 0.81 mg of $Fe_3O_4$ nanoparticles as iron-based additives led to a 39.1% increase in methane generation using canola straw and buffalo dung. Additionally, Zhao, Li, Quan, & Zhang (2017) reported that $Fe_3O_4$ additive in the AD process had a significant impact on biogas yield, with $Fe_3O_4$ nanoparticles ($Fe_3O_4$ NPs), Iron powder, and Iron nanoparticles following suit. These additives also proved beneficial in enhancing substrate digestibility by decomposing lignocellulosic biomass into simpler structures.

While trace elements have proven to be beneficial, their widespread implementation remains limited primarily due to their high cost. To address this issue, and render their utilization economically feasible, more affordable sources of micro-nutrients could be explored (Huiliñir, Montalvo & Guerrero, 2015). Several studies (Huiliñir *et al.,* 2015; Huiliñir, Pinto-Villegas, Castillo, Montalvo, & Guerrero, 2017; Ebrahimi-Nik, Heidari, Azghandi, Mohammadi, & Younesi, 2018) have highlighted the successful utilization of fly ash and drinking water treatment sludge (DWTS). DWTS is composed of alkaline, trace, heavy metals, and clay, arising from the treatment of surface water for drinking purposes. Despite its potential, DWTS is currently disposed of as waste and even requires appropriate disposal methods (Ahmad, Ahmad, & Alam, 2016). In their research, Torres-Lozada *et al.* delved into the impact of adding drinking water sludge to domestic wastewater sludge, aiming to enhance methane production during AD. Their findings revealed that the most favorable mixtures for anaerobic co-digestion should consist of under 20% DWTS (Torres-Lozada, Diaz-Granados & Parra-Orobio, 2015). Ebrahimi-Nik *et al.* (2018) explored the impact of adding DWTS to a mixture of biogas and methane production from food waste. Their findings demonstrated that DWTS additive can lead to a substantial improvement in both biogas and methane yield, up to 65%.

While an optimal dosage of trace elements has been shown to positively impact AD performance, it is crucial to bear in mind that an excessive amount might have adverse effects on the process (Demirel & Scherer, 2011; Schmidt, Nelles, Scholwin & Proter, 2014). Therefore, the application of mathematical modeling in AD proves to be a rapid and cost-effective approach for predicting and optimizing fuel processing engineering and waste industry design (Andriamanohiarisoamanana, Ihara, Yoshida & Umetsu, 2020). In this context, AD processes exhibit compatibility with non-linear models, as the microorganisms' growth and subsequent production kinetics are frequently non-linear (Khamis, 2005). Numerous non-linear regressions (NLRs) were derived from AD experiments, emphasizing the significance of making appropriate selections from an extensive library of functions (Archontoulis & Miguez, 2015). Moreover, it is crucial to ensure that the samples are not only adequately large but also accurately representative to achieve the desired outcomes with the regression model. However, due to the method's high sensitivity, errors may arise (Wang, Tang & Tan, 2011; Wang *et al.,* 2021).

Despite extensive research in the field, there are currently no published studies exploring the potential of enhancing biogas yield by incorporating DWTS into the anaerobic digestion process of dairy manure and comparing it with iron-based additives. Thus, the present project seeks to fill this knowledge gap and aims to model the impact of iron-based additives, namely Fe, $Fe_3O_4$, and DWTS, as trace elements and additives for biogas production during the anaerobic digestion process of dairy manure.

## Materials and Methods

### Materials

The primary feedstock utilized in this study was dairy manure, sourced from the livestock farm of Ferdowsi University of Mashhad, Iran. $Fe_3O_4$ and iron shavings served as the trace elements in this research. The iron shavings, smaller than 1 mm, were procured from the

mechanics laboratory of Ferdowsi University of Mashhad, Iran. To remove oil and impurities, the shavings were immersed in a 14 M sodium hydroxide solution for 24 hours, followed by a day of air drying at room temperature. Additionally, drinking water treatment sludge (DWTS) was obtained from a drinking water treatment plant in Mashhad, Iran, and used as an additive. DWTS, when rich in $Fe_2O_3$, plays a crucial role in municipal water purification. The composition of DWTS used in this research closely resembles the one described in our previous study (Ebrahimi-Nik et al., 2018). The key components of DWTS in descending order include $Fe_2O_3$, $SiO_2$, $CaO$, and $Al_2O_3$. The abundance of $Fe_2O_3$, as revealed by X-ray fluorescence (XRF) analysis, was a result of adding iron chloride as a flocculent during the drinking water treatment process. $SiO_2$ stemmed from the inclusion of suspended solids and various types of clay. Moreover, small quantities of other oxides like $MgO$, $P_2O_5$, $MnO$, $TiO_2$, $P_2O$, and $N_2O$ were identified. DWTS contained trace elements such as Ni, Cr, Co, Zn, Cu, Ba, Sr, Cl, and Zr, detected in parts per million (ppm) levels as well. Before utilization, the sludge underwent air drying and was then ground and passed through specialized sieves to achieve a maximum particle size of 0.63 mm. Additionally, following the methodology outlined in recent studies, microcrystalline cellulose (MERCK-Germany) was prepared as a validation material for inspecting the inoculum's quality (Holliger et al., 2016). To carry out the experiments, a complete stirred tank reactor (CSTR) was employed at Ferdowsi University of Mashhad, Iran, maintaining a stable state and receiving daily feedings of food waste, primarily consisting of rice.

**Data collection and laboratory experimentation**

Conducting the AD process under mesophilic conditions at 37°C, we performed three independent experimental replicates following the procedure outlined by Holliger et al. (2016). The essential inoculum for the AD tests was procured from an active digester within Ferdowsi University of Mashhad's biogas laboratory, which maintained a steady-state operation. To regulate its biogas production rate and ensure suitability for the AD experiments, the collected inoculum underwent 20 days of incubation at 37°C in a warm-water bath (Rosato, 2017).

The experiments were carried out using 500 mL bottles, with a working volume of 400 mL and each bottle's gas-tightness was ensured. To facilitate the gas collection, each bottle was connected to a 2 L gas collection bag via the pneumatic mediator (PUSH-FIT) attached to its lid through a plastic tube. Both the inlet and outlet were present on the gas bags, with a heparin cap connected to the outlet, enabling methane measurement using a syringe. Before sealing the digesters, carbon dioxide was purged over the solution for 30 seconds, establishing anaerobic conditions. Fig. 1 illustrates the experimental setup utilized in this study. The generated biogas was passed through a 7 M sodium hydroxide solution, effectively eliminating impurities and converting them into pure methane (Stoddard, 2010). To maintain a constant temperature of 37°C, a water bath (also known as a bain-marie) was utilized. Additionally, Eq. 1 was employed to determine the suitable materials and their ratios for each bottle.

$$ISR = \frac{V_{in}.VS_{in}}{V_{sub}.VS_{sub}} \tag{1}$$

Where $V_{in}$ represents the volume of inoculum, $VS_{in}$ refers to the VS of inoculum based on wet weight, $V_{sub}$ denotes the volume of substrate, and $VS_{sub}$ represents the VS of the substrate based on wet weight. The ratio of inoculum to substrate (ISR) was adjusted to 5%.
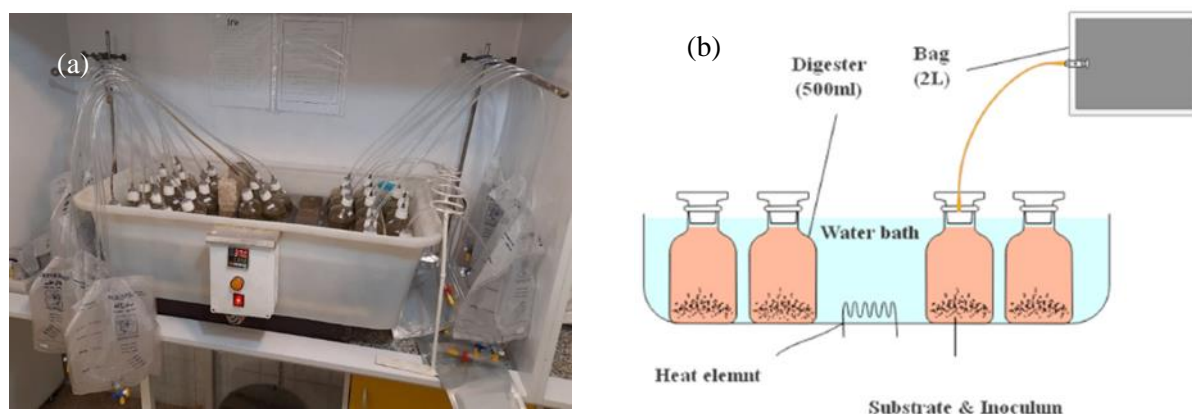
**Fig.1.** Digesters and the Experimental setup (a) photo and (b) schematic illustration

Using a scale with a precision of 0.001 grams, the quantities of each additive were measured. Fe and $Fe_3O_4$ were added at three levels: 10, 20, and 30 mg $L^{-1}$. DWTS was utilized at three concentrations of 6, 12, and 18 mg $L^{-1}$. Table 1 illustrates the experimental treatments and their corresponding symbols, as used in the subsequent section. In this experiment, cellulose was employed as a positive control and combined with the appropriate amount of inoculum to achieve an ISR ratio of 2, with three replicates. Therefore, three bottles containing only inoculum were utilized as control treatments in this study. Consequently, the difference between the methane production of the treated and the control samples ascertains the effect of each treatment on methane production.

Daily measurements of biogas and methane production resulting from the treatments were carried out using a 60cc syringe (Raposo, De la Rubia, Fernández-Cegrí, & Borja, 2012). The anaerobic digestion process spanned 43 days and was concluded when the rate of methane production dropped below 1% of the total cumulative methane production during three consecutive days (Holliger et al., 2016). Throughout this period, the ambient temperature was recorded every day using a mercury thermometer, and the atmospheric pressure data was sourced from the Mashhad synoptic station. These two parameters were crucial for converting the measured biomethane volume into its corresponding standard volume (at standard conditions of temperature T=273.15 K and pressure P=101.325 kPa (Ebrahimzadeh, Ebrahimi-Nik, Rohani & Tedesco, 2021).

**Table 1- Experimental treatment information**

| Additives | Treatment | Unit (mg $L^{-1}$) | Treatment symbol |
|---|---|---|---|
| DWTS | DWTS 6 | 6 | T1 |
|  | DWTS 12 | 12 | T2 |
|  | DWTS 18 | 18 | T3 |
| Fe | Fe 10 | 10 | T4 |
|  | Fe 20 | 20 | T5 |
|  | Fe 30 | 30 | T6 |
| $Fe_3O_4$ | $Fe_3O_4$ 10 | 10 | T7 |
|  | $Fe_3O_4$ 20 | 20 | T8 |
|  | $Fe_3O_4$ 30 | 30 | T9 |

**Measurement of total solids (TS) and volatile solids (VS)**

Throughout and after the experiment, analyses were conducted following established

standards. Specifically, the substrates' total solids (TS) and volatile solids (VS) content were determined before and after the experiments as per the American Standard for Public Health (APHA, 2005). To achieve this, a 50-gram sample comprising various materials used in the experiment (including cellulose, inoculum, and cow manure) was placed in an oven and heated at 105 degrees Celsius for a total of 24 hours. The samples were weighed initially and every hour while in the oven. This process was repeated until the weight of the samples dropped less than 4% in an hour, indicating they had reached a state of constant weight. At this point, the total solids (TS) value was calculated using Eq. 2.

$$TS = \frac{(A - B) \times 100}{(C - B)} \qquad (2)$$

The percentage of total solids (TS) is represented by the variables A, B, and C corresponding to the weight of the dried sample plus petri dish, the petri dish, and the wet sample (substrate) plus petri dish, respectively. To ensure the accuracy of our results, each of these steps was triplicated. The dried materials from the previous step were utilized to calculate the content of volatile solids (VS). For this purpose, a 2-gram sample comprising the mentioned materials was placed inside an oven at a temperature of 550 degrees Celsius for one hour. Then, it was removed and weighed. This process was repeated after another 30 minutes in the oven. The experiment continued until the samples reached a steady state, with a weight change of less than 4% (APHA, 2005) and then VS was calculated using Eq. 3.

$$VS = \frac{(A - D)}{(A - B)} \times 100 \qquad (3)$$

Where VS represents the percentage of total solids, while A, B, and D correspond to the weight of the petri dish plus container, the container alone, and the sample plus container after being heated in an oven, respectively.

**Nonlinear regression analysis of biogas production kinetics**

To examine the production of biogas through the anaerobic digestion of dairy manure and determine the relevant kinetic parameters, nonlinear regression (NLR) models were utilized. Nonlinear regression proves to be a robust instrument for estimating the parameters, including the degradation rate, the gas volume generated per nutrient degradation, and the fermentation process's lag phase of anaerobic digestion (Ebrahimzadeh, Ebrahimi-Nik, Rohani, & Tedesco, 2022). When dealing with unclear or time-dependent associations between the variables in intricate biological systems such as anaerobic digesters, NLR models offer notable advantages. The estimation process in these models incorporates iterative techniques, such as the Levenberg-Marquardt algorithm, which adjusts the model's parameters iteratively to achieve an optimal fit to the data by minimizing the discrepancy between the predicted and actual values. By employing Eq. 4 within the NLR model, the cumulative biogas production (y) as a function of digestion time (t) in the biogas reactor can be effectively assessed. This equation takes into account a random error term (ε), which captures any unexplained variation in the relationship between y and t.

$$y = f(t, \beta) + \varepsilon \qquad (4)$$

To determine the β coefficients that most accurately depict the data, the objective of NLR involves the process of curve fitting. The estimation of these coefficients is usually achieved by minimizing the sum of squared errors (SSE) between the predicted and observed values of the dependent variable. To evaluate the NLR model and its coefficients' importance, researchers often employ the analysis of variance (ANOVA). There are multiple methods of determining NLR model coefficients, and a popular approach is to utilize the Levenberg-Marquardt algorithm, which incorporates a regularization term to prevent overfitting. For our study, the model coefficients were acquired by using the MATLAB function *fitnlm*, which is a built-in function capable of fitting multitudes of NLR models to data. A comprehensive summary of the NLRs analyzed in our study is presented in Table 2. It illustrates the ability to fit an

extensive range of data patterns, including exponential, logarithmic, polynomial, sinusoidal, generalized Mitscherlich, Michael Menten, and power-law functions. NLRs offer a versatile approach to fitting various data patterns.

**Table 2-** Nonlinear regression models for analyzing biogas production from dairy manure

| Name | Equation | Symbol |
|------|----------|--------|
| Logistic-Exponential without LAG | $f(t) = a \dfrac{1 - \exp(-bt)}{1 + \exp\left(\ln\left(\frac{1}{d}\right) - bt\right)}$ | M1 |
| Logistic-Exponential with LAG | $f(t) = a \dfrac{1 - \exp(-b(t - c))}{1 + \exp\left(\ln\left(\frac{1}{d}\right) - b(t - c)\right)}$ | M2 |
| Exponential without LAG | $f(t) = a(1 - \exp(-bt))$ | M3 |
| Exponential with LAG | $f(t) = a(1 - \exp(-b(t - c)))$ | M4 |
| Gompertz | $f(t) = a \exp(-\exp(1 - b(t - c)))$ | M5 |
| Logistic | $f(t) = a \dfrac{1}{1 + \exp(2 + b(c - t))}$ | M6 |
| Generalization of the Mitscherlich | $f(t) = a\left(1 - \exp\left(-b(t - c) - d(\sqrt{t} - \sqrt{c})\right)\right)$ | M7 |
| Michaelis-Menten (MM) | $f(t) = a \dfrac{t^c}{t^c + b^c}$ | M8 |
| Modified MM | $f(t) = a \dfrac{t^c}{t^c + b}$ | M9 |
| Two-pool exponential | $f(t) = \sum_{i=1}^{2} a_i(1 - \exp(-b_i(t - c)))$ | M10 |
| Two-pool logistic | $f(t) = \sum_{i=1}^{2} a_i \dfrac{1}{(1 + \exp(2 - 4b_i(t - c)))}$ | M11 |
| Modified Gompertz | $f(t) = a \exp\left(- \exp\left(2.71 \dfrac{b}{a}(c - t) + 1\right)\right)$ | M12 |
| Logistic | $f(t) = a \dfrac{1}{1 + b\exp(-ct)}$ | M13 |
| Gompertz | $f(t) = a \exp(-b\exp(-ct))$ | M14 |
| Richard | $f(t) = a \dfrac{1}{(1 + b \times \exp(-ct))^{1/d}}$ | M15 |
| Double-Sigmoid | $f(t) = a \dfrac{1}{1 + \exp(-(b + ct + dt^2 + et^3))}$ | M16 |
| Monomolecular- logistic | $f(t) = a(1 - \exp(-bt)) + \dfrac{c}{1 + \exp(-d(t - e))}$ | M17 |
| Chapman-Richard | $f(t) = a(1 - b \times \exp(-ct))^{\left(\frac{1}{1-d}\right)}$ | M18 |
| Exponential-linear | $f(t) = \dfrac{a}{b} \times \ln(1 + \exp(b(t - ct)))$ | M19 |
| LinBiExp | $f(t) = a \times \ln\left(\exp\left(\dfrac{b(t - c)}{d}\right)\right) + \exp\left(\dfrac{e(t - f)}{g}\right) + f$ | M20 |
| Cone | $f(t) = a\left(\dfrac{1}{1 + (bt)^{-c}}\right)$ | M21 |
| Contois | $f(t) = a\left(1 - \dfrac{b}{ct + b - 1}\right)$ | M22 |
| Fitzhugh | $f(t) = a(1 - \exp(-bt)^c)$ | M23 |
| France | $f(t) = \dfrac{a(1 - \exp^{-bt})}{(1 + c\exp^{-bt})}$ | M24 |
| Monod without LAG | $f(t) = a \dfrac{bt}{bt + 1}$ | M25 |
| Monod with LAG | $f(t) = a \dfrac{b(t - c)}{b(t - c) + 1}$ | M26 |

## Criteria for evaluating the fit of nonlinear regression models

To assess the goodness-of-fit of nonlinear regression models, we employed Eq. 5 representing the coefficient of determination ($R^2$), Eq. 6 for calculating root mean square error (RMSE), and the minimum value predicted by the model (MP). The process of identifying the most fitting models was facilitated through the application of these criteria, and we were able to identify the models that most precisely depict the fundamental biogas production kinetics using them.

$$R^2 = 1 - \frac{\sum_1^N (B_{ai} - \hat{B}_{pi})^2}{\sum_1^N (B_{ai} - \overline{B_a})^2} \qquad (5)$$

$$RMSE = \sqrt{\sum_{i=1}^n \frac{\left| B_{ai} - \hat{B}_{pi} \right|^2}{N}} \qquad (6)$$

Where $B_a$ and $B_p$ denote the experimental and predicted values, respectively. The $\overline{B_a}$ represents the average value of the experimental values, and N denotes the sample size. When selecting the best model, a good fit with experimental data is indicated by a low RMSE value and a high $R^2$ value. Because biogas production originates from zero at the start of the digestion process, the fitted model must also pass through the origin of coordinates. The model's physical interpretability and validity for predicting future biogas yields are ensured with this crucial requirement. In other words, the requirement of passing through the origin of the coordinates is crucial to guarantee the model's physical interpretability and validity for future biogas yield predictions.

## Results and Discussions

This section focuses on evaluating the performance of non-linear regression models applied to the cumulative methane data gathered throughout the anaerobic digestion process. Furthermore, a comparison is made between the gas production rates and the average cumulative methane produced using the various treatments.

## Finding the best-fit non-linear regression model

Accurate analysis of the cumulative methane data obtained during the anaerobic digestion process relies on selecting the most appropriate non-linear regression model. One crucial criterion for this selection is the model's ability to cross the origin of the coordinates, ensuring that it estimates a value of zero at the beginning of the digestion process. This property ensures that the model is consistent with the actual process. In Table 3, we present the predicted cumulative methane production at the start of the anaerobic digestion process for 26 non-linear regression models. Through our evaluation, out of the 26 models, we identified eight valid models that met this property. While some other models, like M22, M13, and M2, could predict zero values for specific treatments only; making them unsuitable for our analysis. Consequently, we excluded these models from further consideration and focused on the ones predicting a zero value for all treatments. Thus, we narrowed down our selection to these eight models for further analysis. In the subsequent sections, we will discuss the performance of these eight models and compare their results to identify the best-fit model for analyzing the cumulative methane data.

**Table 3-** Predicted minimum amounts of methane produced during the digestion time for the studied treatments, utilizing 26 non-linear regression models

| Model | T1 | T2 | T3 | T4 | T5 | T6 | T7 | T8 | T9 |
|-------|------|------|------|------|------|------|------|------|-------|
| M1 | 0.00 | 0.00 | 0.00 | 0.00 | 0.00 | 0.00 | 0.00 | 0.00 | 0.00 |
| M2 | -190 | -203 | -162 | -16 | -44 | 0 | 0.00 | 0.00 | 0.00 |
| M3 | 0.00 | 0.00 | 0.00 | 0.00 | 0.00 | 0.00 | 0.00 | 0.00 | 0.00 |
| M4 | -155 | -222 | -132 | -14 | -197 | -75 | -251 | -132 | -40 |
| M5 | 100 | 46 | 65 | 31 | 33 | 22 | 0.00 | 0.00 | 0.00 |
| M6 | 263 | 165 | 202 | 47 | 109 | 46 | 14 | 3 | 21 |
| M7 | -155 | -226 | -171 | -21 | -194 | -80 | -154 | -96 | -41 |
| M8 | 0.00 | 0.00 | 0.00 | 0.00 | 0.00 | 0.00 | 0.00 | 0.00 | 0.00 |
| M9 | 0.00 | 0.00 | 0.00 | 0.00 | 0.00 | 0.00 | 0.00 | 0.00 | 0.00 |
| M10 | -97 | -90 | -73 | -65 | -70 | -69 | -44 | -48 | -57 |
| M11 | 97 | 0 | 91 | 66 | 6 | 6 | 54 | 45 | 77 |
| M12 | 100 | 46 | 65 | 31 | 33 | 22 | 0.00 | 0.00 | 0.00 |
| M13 | 1 | 1 | 1 | 0 | 1 | 3 | 0.00 | 0.00 | 0.00 |
| M14 | 100 | 46 | 65 | 34 | 33 | 22 | 0.00 | 14 | 18 |
| M15 | 89 | 49 | 82 | 40 | 33 | 21 | 1 | 0.00 | 28.48 |
| M16 | 1124 | 1055 | 886 | 413 | 712 | 582 | 633 | 432 | 352 |
| M17 | 1.27 | 0.00 | 0.00 | 1.69 | 0.00 | 3.57 | 2 | 0.00 | 0.00 |
| M18 | 58 | 63 | 59 | 3 | 60 | 68 | 15 | 6 | 9 |
| M19 | 1039 | 1022 | 845 | 29 | 747 | 728 | 7 | 5 | 32 |
| M20 | 347 | 258 | 347 | 50 | 330 | 318 | 38 | 58 | 106 |
| M21 | 0.00 | 0.00 | 0.00 | 0.00 | 0.00 | 0.00 | 0.00 | 0.00 | 0.00 |
| M22 | 0 | 0 | 0 | 0 | 0 | 0 | 0 | 0 | -150 |
| M23 | 0.00 | 0.00 | 0.00 | 0.00 | 0.00 | 0.00 | 0.00 | 0.00 | 0.00 |
| M24 | 0.00 | 0.00 | 0.00 | 0.00 | 0.00 | 0.00 | 0.00 | 0.00 | 0.00 |
| M25 | 924 | 951 | 803 | 286 | 686 | 645 | 471 | 322 | 284 |
| M26 | 0.00 | 0.00 | 0.00 | 0.00 | 0.00 | 0.00 | 0.00 | 0.00 | 0.00 |

In Table 4, the results of RMSE and $R^2$ for each of the nine treatments are presented. Based on the $R^2$ criterion, we observed that four models (M9, M21, M24, and M26) lacked sufficient predictive ability to estimate cumulative methane production during the digestion process, as their $R^2$ values were the lowest. Among the remaining four models, the Michaelis-Menten model (M8) demonstrated superior predictive ability for all treatments. Although the M1 model also exhibited good predictive ability, we excluded it from the selection list due to its complexity in comparison to the M8 model. Consequently, we proceeded with the Michaelis-Menten non-linear regression model (M8) for further analyses, which will be presented in the following sections.

Iron-based additives exhibited diverse behaviors during the biodegradation process of dairy manure. Although the First-order and Gompertz models are commonly used for monitoring biodegradation in anaerobic

digestion (AD) processes, they were not found to be adequately suitable for modeling the AD of dairy manure with iron-based additives. The biodegradation of starch-based bioplastic under anaerobic conditions was evaluated to determine an appropriate kinetic model. The analysis involved examining 26 nonlinear regression models, and it was found that the modified Michaelis-Menten (MM) model was the best-fitted model for the biodegradation process (Ebrahimzadeh *et al.,* 2022). The innovative multi-Gompertz model has been proposed as the most suitable model for biogas production from residual marine macroalgae biomass (Pardilhó, Pires, Boaventura, Almeida & Dias, 2022). Additionally, other models are employed for more specific conditions and additives, such as higher solids contents (e.g., Chen and Hashimoto model), or specific microorganisms (e.g., cone model) (Karki *et al.,* 2022; Lima, Adarme, Baˆeta, Gurgel, & de Aquino, 2018; Masih-Das & Tao, 2018).

**Table 4-** Assessment of eight selected non-linear regression models using RMSE and $R^2$ criteria

| | | T1 | T2 | T3 | T4 | T5 | T6 | T7 | T8 | T9 |
|---|---|---|---|---|---|---|---|---|---|---|
| M1 | RMSE | 118 | 137 | 139 | 189 | 139 | 142 | 92 | 87 | 79 |
| | $R^2$ | 0.97 | 0.96 | 0.95 | 0.75 | 0.92 | 0.87 | 0.97 | 0.94 | 0.92 |
| M3 | RMSE | 118 | 149 | 140 | 190 | 150 | 145 | 534 | 138 | 108 |
| | $R^2$ | 0.97 | 0.95 | 0.95 | 0.74 | 0.90 | 0.86 | 0.00 | 0.85 | 0.85 |
| M8 | RMSE | 90 | 118 | 130 | 187 | 134 | 138 | 91 | 85 | 81 |
| | $R^2$ | 0.98 | 0.97 | 0.95 | 0.75 | 0.92 | 0.87 | 0.97 | 0.94 | 0.92 |
| M9 | RMSE | 674 | 963 | 130 | 471 | 746 | 574 | 709 | 450 | 325 |
| | $R^2$ | 0.11 | 0.00 | 0.95 | 0.00 | 0.00 | 0.00 | 0.00 | 0.00 | 0.00 |
| M13 | RMSE | 288 | 254 | 257 | 247 | 202 | 163 | 119 | 102 | 88 |
| | $R^2$ | 0.84 | 0.86 | 0.82 | 0.57 | 0.82 | 0.82 | 0.95 | 0.92 | 0.90 |
| M21 | RMSE | 1318 | 1256 | 1063 | 367 | 805 | 630 | 625 | 319 | 191 |
| | $R^2$ | 0.00 | 0.00 | 0.00 | 0.00 | 0.00 | 0.00 | 0.00 | 0.21 | 0.53 |
| M24 | RMSE | 1321 | 1259 | 1066 | 375 | 807 | 633 | 634 | 341 | 214 |
| | $R^2$ | 0.00 | 0.00 | 0.00 | 0.00 | 0.00 | 0.00 | 0.00 | 0.10 | 0.41 |
| M26 | RMSE | 553 | 528 | 454 | 321 | 362 | 277 | 480 | 320 | 244 |
| | $R^2$ | 0.40 | 0.39 | 0.43 | 0.27 | 0.44 | 0.49 | 0.13 | 0.20 | 0.24 |

Table 5 presents the coefficients of the Michaelis-Menten nonlinear regression model, along with their standard deviation, p-values, coefficient of determination ($R^2$), and the adjusted coefficient of determination for each of the studied treatments. The p-value is equal to zero in all cases, indicating that the coefficients of the models are statistically significant at a significance level of one percent. The small standard deviation values of the coefficients, relative to the coefficient values, provide further evidence that the models' estimations can be trusted. Except for the T4 treatment, all other treatments have an $R^2$ value equal to or greater than 0.93, confirming the prediction reliability of the models. Hence, the results will be interpreted based on the estimations of the models.

**Table 5-** Coefficients, significance results, and coefficient of determination values for the Michaelis-Menten model

| | | T1 | T2 | T3 | T4 | T5 | T6 | T7 | T8 | T9 |
|---|---|---|---|---|---|---|---|---|---|---|
| Coefficients | a | 2566.0 | 2280.0 | 2158.5 | 1275.3 | 1562.9 | 1273.9 | 1325.3 | 893.0 | 736.1 |
| | b | 1.64 | 1.95 | 1.59 | 1.56 | 1.98 | 2.37 | 5.06 | 5.77 | 5.35 |
| | c | 11.50 | 9.83 | 10.76 | 17.46 | 8.41 | 6.50 | 13.31 | 12.90 | 12.62 |
| Std | a | 50.95 | 38.94 | 71.30 | 208.83 | 34.37 | 24.16 | 12.70 | 9.94 | 12.25 |
| | b | 0.07 | 0.10 | 0.12 | 0.35 | 0.16 | 0.26 | 0.29 | 0.44 | 0.59 |
| | c | 0.37 | 0.27 | 0.60 | 4.39 | 0.34 | 0.30 | 0.17 | 0.19 | 0.29 |
| p-value | a | 0.00 | 0.00 | 0.00 | 0.00 | 0.00 | 0.00 | 0.00 | 0.00 | 0.00 |
| | b | 0.00 | 0.00 | 0.00 | 0.00 | 0.00 | 0.00 | 0.00 | 0.00 | 0.00 |
| | c | 0.00 | 0.00 | 0.00 | 0.00 | 0.00 | 0.00 | 0.00 | 0.00 | 0.00 |
| $R^2$ | $R^2$ | 0.99 | 0.98 | 0.97 | 0.80 | 0.96 | 0.93 | 0.98 | 0.97 | 0.94 |
| | $R^2_{Adj.}$ | 0.99 | 0.98 | 0.97 | 0.80 | 0.95 | 0.92 | 0.98 | 0.97 | 0.94 |

For a deeper understanding of the impact of coefficients in the Michaelis-Menten nonlinear regression model, a sensitivity analysis was conducted. Insights were gained by plotting the methane production trend during the digestion process and altering a single

coefficient at a time; the others were kept constant at their average values. The results of this analysis are presented in Fig. 2. The regression coefficient 'a' has a direct influence on the maximum methane production during the digestion process. Higher values of 'a' increased methane production, while lower values resulted in lower production. This coefficient represents the horizontal asymptote of the methane production curve. On the other hand, coefficient 'b' governs the slope of the methane production curve, impacting the time it takes to reach maximum methane production. A higher value of 'b' leads to a steeper slope and the methane production reaches its maximum more quickly. Conversely, an increase in coefficient 'c' slows down the rate of methane production, and requires a longer time to reach the maximum production level. Considering the behavior of these three regression coefficients, it can be concluded that the highest amount of methane production occurs when coefficients 'a' and 'b' are high, and coefficient 'c' is low. This combination results in faster methane production over a shorter period.
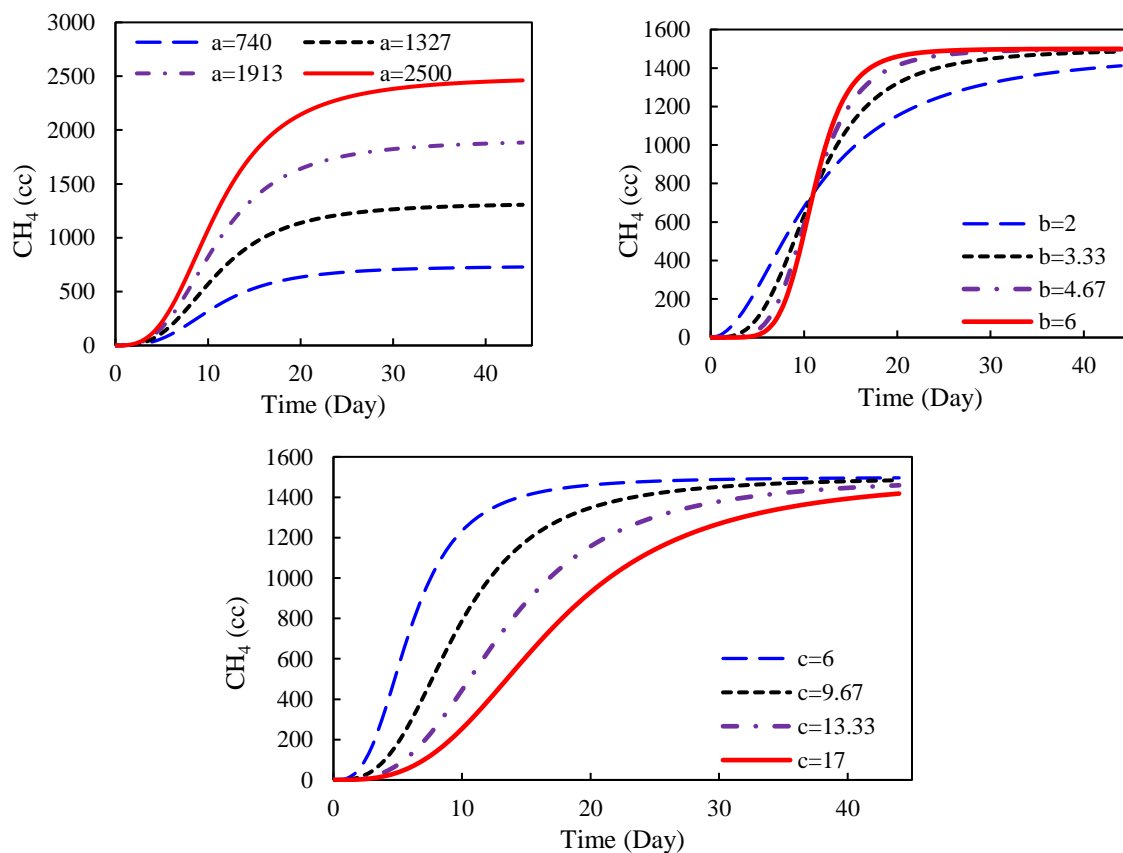


**Fig.2.** Sensitivity analysis investigating the effect of the Michaelis-Menten model coefficients a, b, and c on methane production

Fig. 3 presents the fitting outcomes of the Michaelis-Menten nonlinear regression model for all of the investigated treatments, along with the upper and lower limits of the fitted curve. The results indicate variations in the dispersion of experimental data among the different treatments, likely due to differences in experimental conditions. Nevertheless, considering the proximity of the upper and lower limits of the fitted curve and the model evaluation, it can be inferred that the fitted results effectively represent the variability of methane production within the studied treatments.
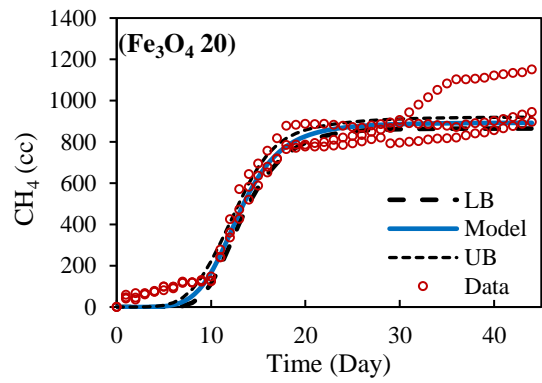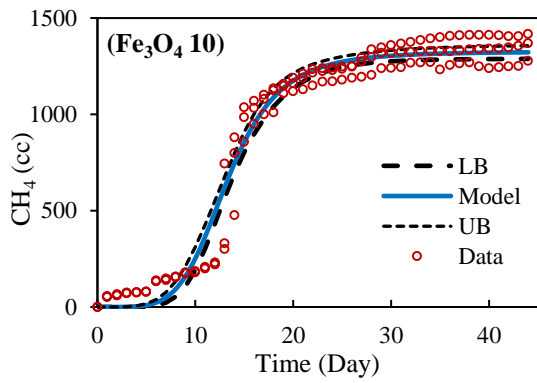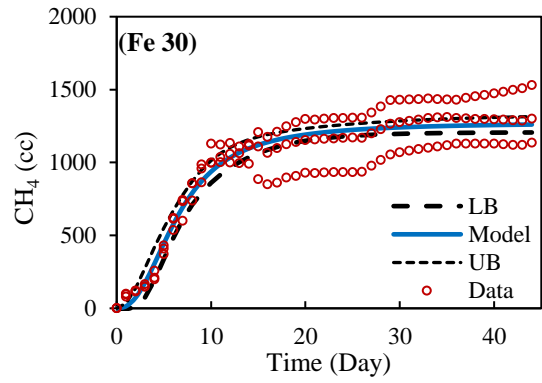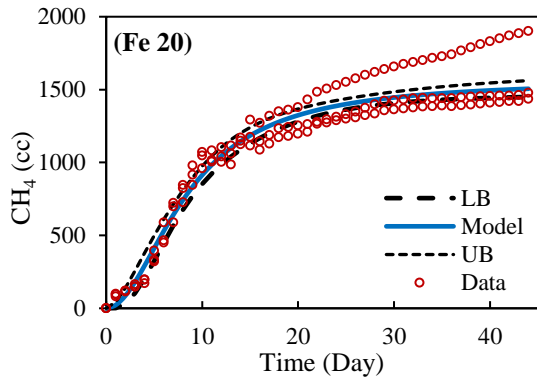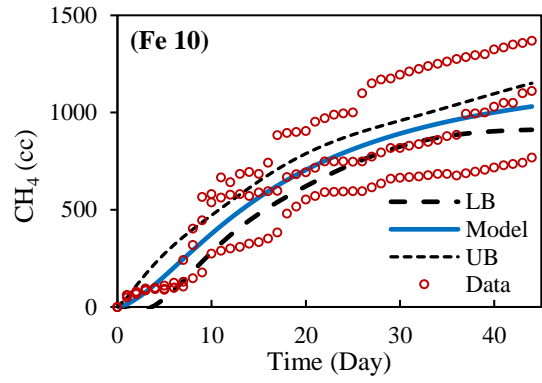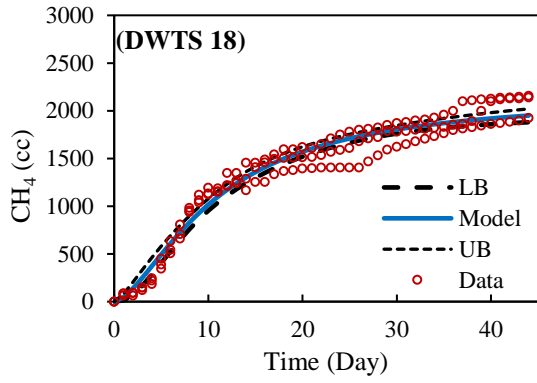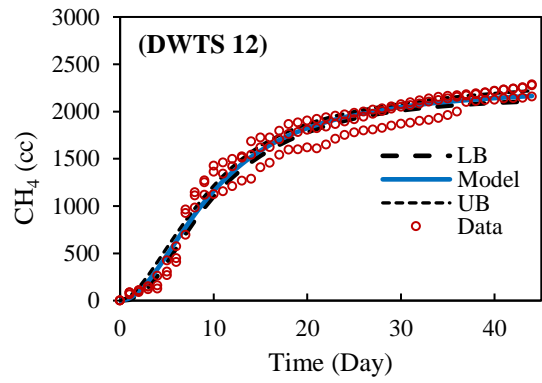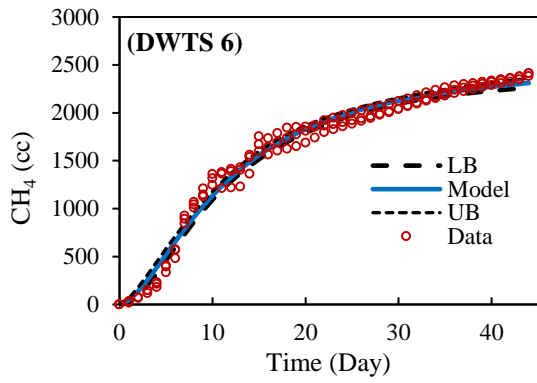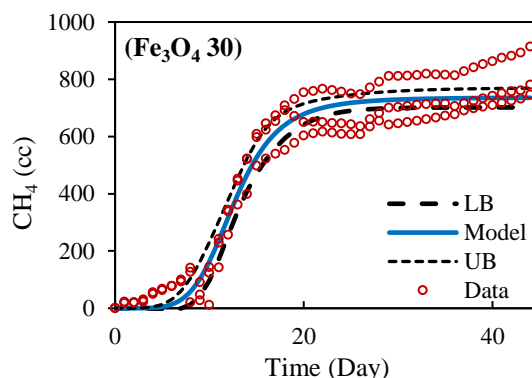
**Fig.3.** Curve fitting of the Michaelis-Menten nonlinear regression model for each of the studied treatments, showing the dispersion of experimental data and the upper (UB) and lower (LB) bounds of the fit

The final amount of methane production and its changes during the process were compared using non-linear regression models, as depicted in Fig. 4. Among the studied treatments, DWTS6, DWTS12, and DWTS18 showed the highest levels of methane production, while $Fe_3O_4 20$ and $Fe_3O_4 30$ resulted in the lowest levels. The maximum methane production for DWTS6 was approximately 34% and 42% higher than that of Fe20 and $Fe_3O_4 30$, respectively, which were the best-performing levels among the Fe additives' treatments. This indicates that DWTS acts as a mixture of different trace elements with synergistic and antagonistic effects, resulting in an enhancement of methane production from dairy manure. Previous research by Ebrahimi-Nik *et al.* (2018) demonstrated that the addition of 6 mg/kg DWTS to the anaerobic digestion of food waste, compared to the control digester, resulted in a significant increase of 65% and 58% in biogas and methane yields, respectively. In Fig. 4 it is evident that until the 10th day of the digestion process, $Fe_3O_4 10$ produced less methane than all levels of Fe. However, after the twelfth day, the methane production rapidly exceeded all levels of Fe, indicating a unique pattern of methane generation for $Fe_3O_4 10$ compared to other levels of Fe. The addition of $Fe_3O_4$ to the anaerobic digestion (AD) process has been reported to have a significant positive effect on

biogas yield. These additives also contribute to improving substrate digestibility by facilitating the decomposition of lignocellulosic biomass into simpler structures (Zhao *et al.,* 2017). Ali, Mahar, Soomro, & Sherazi (2017) observed a remarkable 72.1% increase in methane content when using municipal solid waste (MSW) as a substrate for the AD process with the addition of $Fe_3O_4$ nanoparticles. In another study, Abdelsalam *et al.* (2017) investigated the impact of iron nanoparticles and iron oxide nanoparticles on biogas and methane production using cattle dung slurry and found that $Fe_3O_4$ NPs with a concentration of 20 mg/L led to a substantial 65.6% increase in biogas production. $Fe_3O_4$ NPs additives have also been associated with the highest biogas yield reported from an AD process (Casals *et al.,* 2014). These findings highlight the potential and significance of $Fe_3O_4$-based additives in enhancing biogas production in anaerobic digestion processes. Regarding the slope of methane production, it is observed that the top two treatments, DWTS6 and DWTS12, have the same slope until day 20. However, after day 20, the methane production trend for DWTS6 rises above that of DWTS12. Generally, the slope of methane production varies among different treatments, with some showing an uphill start, which may also have a significant impact on their overall methane production.
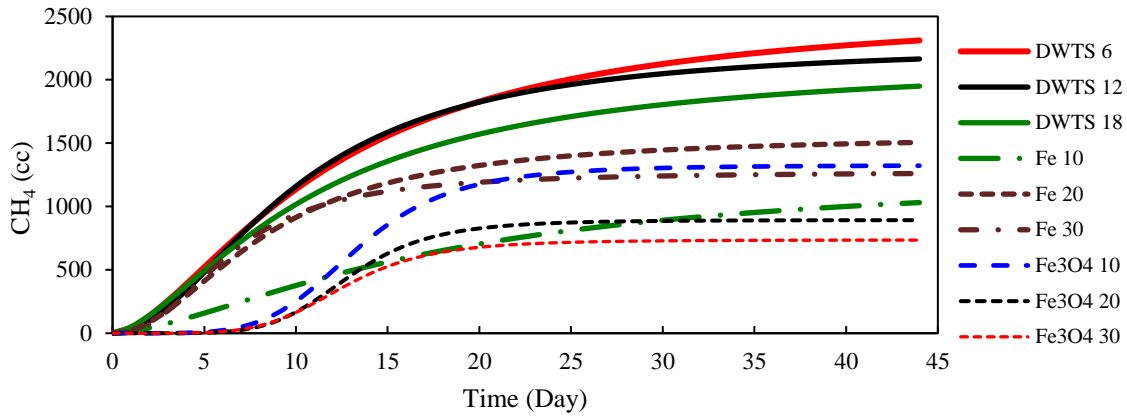
**Fig.4**. Methane production during the anaerobic digestion process using non-linear regression models for each of the treatments
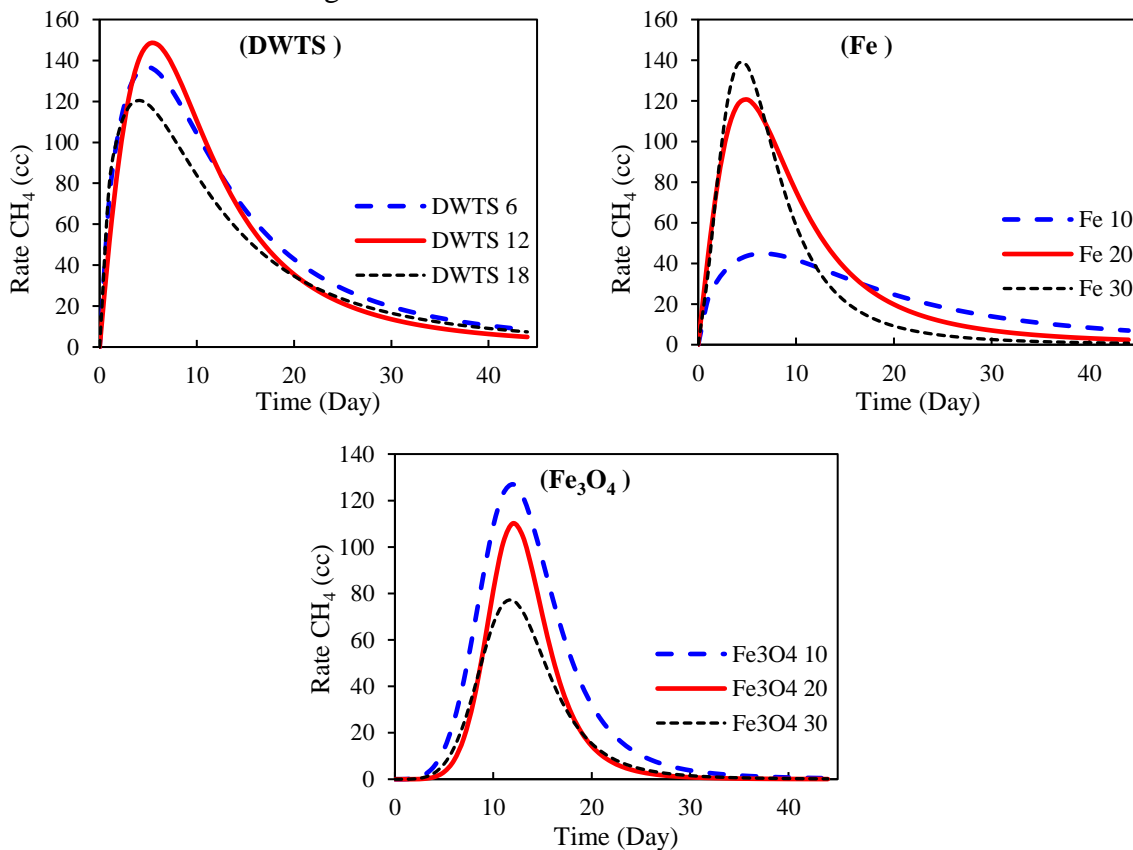


**Fig.5.** Changes in the production rate of methane during the anaerobic digestion process using a non-linear regression model for each of the three additives

Fig. 5 displays the methane production rate from the treatments throughout 40 days. Sigmoid gas production curves can be categorized into three stages: the initial stage with slow or no gas production, the rapid gas production stage (exponential stage), and the final stage where gas production slows down and eventually reaches zero (asymptotic stage). A comparison of the three types of treatments reveals that only the treatments with different levels of $Fe_3O_4$ experienced an initial stage. Consequently, these treatments

reached their maximum production rate after day ten, while other additives (DWTS and Fe) achieved their maximum rates before the 10th day. It was observed that a higher level of $Fe_3O_4$ corresponds to a lower methane production rate in all three stages. However, Fe20 and Fe30 exhibited increased methane rates in the first two stages. It is noteworthy that the lower level of Fe (Fe20) resulted in a higher methane production rate than Fe30 at the end of the process, particularly after the 18th day and during the third stage. When comparing different levels of DWTS, it was evident that although these treatments had similar rates during the first and final days of the process, DWTS12 exhibited the highest methane production rate during the rapid gas production stage. Specifically, the maximum methane production rate of DWTS12 in the second stage was approximately 5% and 22% higher than DWTS6 and DWTS18, respectively.

Abdelsalam et al. (2017) conducted a study on the impact of magnetic iron oxide nanoparticles on methane production from anaerobic digestion of manure. Their findings revealed that utilizing 20 mg $L^{-1}$ of $Fe_3O_4$ resulted in the highest methane production

rate, surpassing the rates observed with 5 mg $L^{-1}$ and 10 mg $L^{-1}$ of $Fe_3O_4$. The maximum methane production rate was achieved before the 5th day and reached approximately 110 cc for the AD process of food waste when 6 mg $L^{-1}$ of DWTS was used. This result aligns closely with the findings obtained for the same treatment in one of our other studies (Ebrahimzadeh et al., 2022).

Using the results obtained from the modeling analysis, we computed the quantity of methane production for each of the nine treatments at various points during the anaerobic digestion process. We calculated methane production when it reached 25%, 50%, 75%, and 90% of the final amount achieved at the end of the process. The computed values for T25, T50, T75, and T90 of each treatment are presented in Table 6. By examining these values for the treatments, we can determine the speed at which each treatment achieves its maximum methane production. Opting for a treatment that reaches its maximum methane production earlier with a higher percentage would be preferable, as it indicates a more efficient and effective process.

**Table 6-** Calculated methane production values for T25, T50, T75, and T90 for each treatment

| Additive | Treatment | T25 (day) | T50 (day) | T75 (day) | T90 (day) |
|---|---|---|---|---|---|
| DWTS | DWTS 6 | 5.65 | 11.29 | 21.77 | 38.89 |
| | DWTS 12 | 5.64 | 9.65 | 16.32 | 26.93 |
| | DWTS 18 | 5.28 | 9.40 | 16.49 | 28.03 |
| Fe | Fe 10 | 8.48 | 17.65 | 23.05 | 32.61 |
| | Fe 20 | 4.73 | 7.94 | 13.20 | 21.57 |
| | Fe 30 | 4.21 | 6.64 | 10.41 | 16.14 |
| $Fe_3O_4$ | $Fe_3O_4$ 10 | 10.41 | 13.22 | 16.72 | 21.06 |
| | $Fe_3O_4$ 20 | 10.76 | 13.02 | 15.71 | 18.90 |
| | $Fe_3O_4$ 30 | 10.40 | 12.16 | 14.20 | 16.53 |

Notes: T25, T50, T75, and T90 represent the times when methane production reaches 25%, 50%, 75%, and 90% of the maximum amount achieved at the end of the anaerobic digestion process, respectively.

Lastly, Fig. 6 presents the comparison of average cumulative methane production among the studied treatments using the LSD method after the completion of the anaerobic digestion process. Notably, the figure highlights a significant difference ($P > 0.05$) in biomethane production between the different levels of DWTS, Fe, and $Fe_3O_4$. It can be seen

that the treatment with DWTS6 exhibits the highest level of average cumulative methane production, and there is a statistically significant difference between this treatment and all the others, except DWTS12. This suggests that DWTS6 stands out as a particularly effective treatment for promoting methane production during the anaerobic

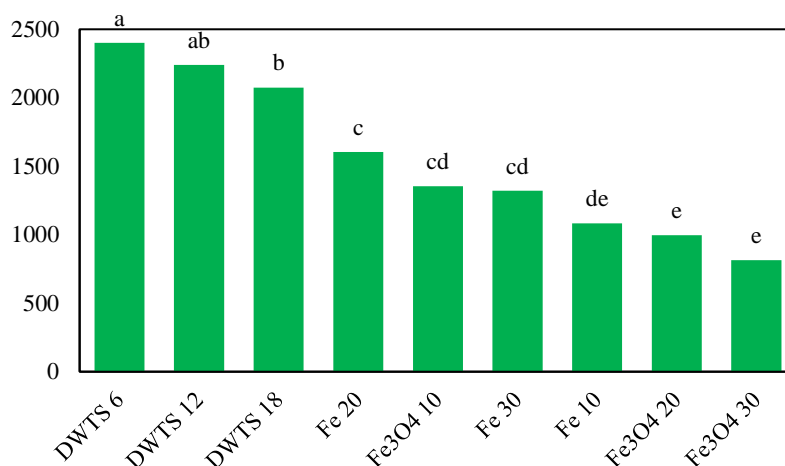digition process, warranting further consideration for practical applications.



**Fig.6.** Comparison of average cumulative methane production among the treatments using the LSD method at 5% level after completion of the anaerobic digestion process

## Conclusion

In this study, we investigated the impact of iron-based additives, including Fe, $Fe_3O_4$, and DWTS, at three levels, on the anaerobic digestion of dairy manure. Additionally, we introduced and evaluated 26 different non-linear models to better understand the kinetics of methane production from the AD process. Among these models, the Michaelis-Menten model (M8) demonstrated the best performance in estimating the methane production kinetics for all nine treatments over time.

The results revealed that different levels of DWTS exhibited the highest methane production compared to various levels of Fe and $Fe_3O_4$. Interestingly, $Fe_3O_4$ at level 30 displayed the lowest biomethane production among all the $Fe_3O_4$ treatments. Moreover, DWTS at level 6 achieved the highest average cumulative methane production among the studied treatments using the LSD method at a 5% significance level after the completion of the anaerobic digestion process.

The methane production rate for treatments with DWTS and Fe reached its maximum before the 5th day, while in $Fe_3O_4$ treatments, it occurred around the 12th day. Additionally,

while higher levels of Fe increased the methane production rate, increasing the level of $Fe_3O_4$ showed the opposite effect. Notably, among all the treatments, DWTS at level 12 displayed the highest maximum methane production rate, peaking at approximately 147.6 cc on the 6th day.

These findings provide valuable insights into the kinetics of anaerobic digestion of dairy manure. However, further research is required to determine whether these results can be applied to other types of livestock manure as well. Future studies could involve applying the proposed models to different datasets to validate and refine our understanding of the anaerobic digestion process.

## Acknowledgment

## Conflict of Interest

The authors declare that they have no conflict of interest.

## References

1. Abdelsalam, E., Samer, M., Attia, Y., Abdel-Hadi, M., Hassan, H., & Badr, Y. (2016). Comparison of nanoparticles effects on biogas and methane production from anaerobic digestion of cattle dung slurry. *Renewable Energy, 87*, 592-598. https://doi.org/10.1016/j.renene.2015.10.053

2. Abdelsalam, E., Samer, M., Attia, Y. A., Abdel-Hadi, M. A., Hassan, H. E., & Badr, Y. (2017). Influence of zero valent iron nanoparticles and magnetic iron oxide nanoparticles on biogas and methane production from anaerobic digestion of manure. *Energy*, *120*, 842-853. https://doi.org/10.1016/j.energy.2016.11.137

3. Ahmad, T., Ahmad, K., & Alam, M. (2016). Sustainable management of water treatment sludge through 3 'R'concept. *Journal of Cleaner Production, 124*, 1-13. https://doi.org/10.1016/j.jclepro.2016.02.073

4. Al Seadi, T., Rutz, D., Prassl, H., Köttner, M., Finsterwalder, T., Volk, S., & Janssen, R. (2008). Biogas Handbook; University of Southern Denmark Esbjerg: Esbjerg, Denmark, 2008. Google Scholar.

5. Ali, A., Mahar, R. B., Soomro, R. A., & Sherazi, S. T. H. (2017). $Fe_3O_4$ nanoparticles facilitated anaerobic digestion of organic fraction of municipal solid waste for enhancement of methane production. *Energy Sources, Part A: Recovery, Utilization, and Environmental Effects, 39*(16), 1815-1822. https://doi.org/10.1080/15567036.2017.1384866

6. Andriamanohiarisoamanana, F. J., Ihara, I., Yoshida, G., & Umetsu, K. (2020). Kinetic study of oxytetracycline and chlortetracycline inhibition in the anaerobic digestion of dairy manure. *Bioresource Technology, 315*, 123810. https://doi.org/10.1016/j.biortech.2020.123810

7. APHA. (2005). Standard Methods for the Examination of Water and Wastewater. 21st ed. American Public Health Association, Washington DC, 1220p.

8. Archontoulis, S. V., & Miguez, F. E. (2015). Nonlinear regression models and applications in agricultural research. *Agronomy Journal, 107*(2), 786-798. https://doi.org/10.2134/agronj2012.0506

9. Casals, E., Barrena, R., Garcia, A., González, E., Delgado, L., Busquets-Fité, M., Font Segura, X., Arbiol, J., Glatzel, P., Kvashnina, K., Sánchez, A., & Puntes, V. (2014). Programmed Iron Oxide Nanoparticles Disintegration in Anaerobic Digesters Boosts Biogas Production. Small (Weinheim an Der Bergstrasse, Germany), 10. https://doi.org/10.1002/smll.201303703

10. Chen, R., Konishi, Y., & Nomura, T. (2018). Enhancement of methane production by Methanosarcina barkeri using $Fe_3O_4$ nanoparticles as iron sustained release agent. *Advanced Powder Technology, 29*(10), 2429-2433. https://doi.org/10.1016/j.apt.2018.06.022

11. Cheng, J., Zhu, C., Zhu, J., Jing, X., Kong, F., & Zhang, C. (2020). Effects of waste rusted iron shavings on enhancing anaerobic digestion of food wastes and municipal sludge. *Journal of Cleaner Production*, *242*, 118195. https://doi.org/10.1016/j.jclepro.2019.118195

12. Choong, Y. Y., Norli, I., Abdullah, A. Z., & Yhaya, M. F. (2016). Impacts of trace element supplementation on the performance of anaerobic digestion process: A critical review. *Bioresource Technology, 209*, 369-379. https://doi.org/10.1016/j.biortech.2016.03.028

13. Demirel, B., & Scherer, P. (2011). Trace element requirements of agricultural biogas digesters during biological conversion of renewable biomass to methane. *Biomass and Bioenergy, 35*(3), 992-998. https://doi.org/10.1016/j.biombioe.2010.12.022

14. Dudley, B. (2019). *BP statistical review of world energy 2016*. British Petroleum Statistical Review of World Energy, Bplc. editor, Pureprint Group Limited, UK.

15. Ebrahimi-Nik, M., Heidari, A., Azghandi, S. R., Mohammadi, F. A., & Younesi, H. (2018). Drinking water treatment sludge as an effective additive for biogas production from food waste; kinetic evaluation and biomethane potential test. *Bioresource Technology, 260*, 421-426. https://doi.org/10.1016/j.biortech.2018.03.112

16. Ebrahimzade, I., Ebrahimi-Nik, M., Rohani, A., & Tedesco, S. (2021). Higher energy conversion efficiency in anaerobic degradation of bioplastic by response surface methodology. *Journal of Cleaner Production, 290*, 125840. https://doi.org/10.1016/j.jclepro.2021.125840

17. Ebrahimzade, I., Ebrahimi-Nik, M., Rohani, A., & Tedesco, S. (2022). Towards monitoring biodegradation of starch-based bioplastic in anaerobic condition: Finding a proper kinetic model. *Bioresource Technology, 347*, 126661. https://doi.org/10.1016/j.biortech.2021.126661

18. Gkotsis, P., Kougias, P., Mitrakas, M., & Zouboulis, A. (2023). Biogas upgrading technologies–Recent advances in membrane-based processes. *International Journal of Hydrogen Energy, 48*(10), 3965-3993. https://doi.org/10.1016/j.ijhydene.2022.10.228

19. Hao, X., Wei, J., van Loosdrecht, M. C., & Cao, D. (2017). Analysing the mechanisms of sludge digestion enhanced by iron. *Water Research, 117*, 58-67. https://doi.org/10.1016/j.watres.2017.03.048

20. Holliger, C., Alves, M., Andrade, D., Angelidaki, I., Astals, S., Baier, U., Bougrier, C., Buffière, P., Carballa, M., & De Wilde, V. (2016). Towards a standardization of biomethane potential tests. *Water Science and Technology, 74*(11), 2515-2522. https://doi.org/10.2166/wst.2016.336

21. Huiliñir, C., Montalvo, S., & Guerrero, L. (2015). Biodegradability and methane production from secondary paper and pulp sludge: effect of fly ash and modeling. *Water Science and Technology, 72*(2), 230-237. https://doi.org/10.2166/wst.2015.210

22. Huiliñir, C., Pinto-Villegas, P., Castillo, A., Montalvo, S., & Guerrero, L. (2017). Biochemical methane potential from sewage sludge: Effect of an aerobic pretreatment and fly ash addition as source of trace elements. *Waste Management, 64*, 140-148. https://doi.org/10.1016/j.wasman.2017.03.023

23. Karki, R., Chuenchart, W., Surendra, K. C., Sung, S., Raskin, L., & Khanal, S. K. (2022). Anaerobic co-digestion of various organic wastes: Kinetic modeling and synergistic impact evaluation. *Bioresource Technology, 343*, 126063. https://doi.org/10.1016/j.biortech.2021.126063

24. Khamis, A. (2005). Nonlinear growth models for modeling oil palm yield growth. *Journal of Mathematics and Statistics, 1*(3), 225-233. https://doi.org/10.3844/jmssp.2005.225.232

25. Kong, X., Yu, S., Xu, S., Fang, W., Liu, J., & Li, H. (2018). Effect of FeO addition on volatile fatty acids evolution on anaerobic digestion at high organic loading rates. *Waste Management, 71*, 719-727. https://doi.org/10.1016/j.wasman.2017.03.019

26. Lima, D. R. S., Adarme, O. F. H., Baˆeta, B. E. L., Gurgel, L. V. A., & de Aquino, S. F. (2018). Influence of different thermal pretreatments and inoculum selection on the biomethanation of sugarcane bagasse by solid-state anaerobic digestion: A kinetic analysis. *Industrial Crops and Products, 111*, 684-693. https://doi.org/10.1016/j.indcrop.2017.11.048

27. Lu, J., & Gao, X. (2021). Biogas: Potential, challenges, and perspectives in a changing China. *Biomass and Bioenergy, 150*, 106127. https://doi.org/10.1016/j.biombioe.2021.106127

28. Muddasar, M. (2022). Biogas production from organic wastes and iron as an additive–a short review. Preprints.org 2022, 2022010026. https://doi.org/10.20944/preprints202201.0026.v1

29. Masih-Das, J., & Tao, W. (2018). Anaerobic co-digestion of foodwaste with liquid dairy manure or manure digestate: Co-substrate limitation and inhibition. *Journal of Environmental Management, 223*, 917-924. https://doi.org/10.1016/j.jenvman.2018.07.016

30. Noonari, A. A., Mahar, R. B., Sahito, A. R., & Brohi, K. M. (2019). Anaerobic co-digestion of canola straw and banana plant wastes with buffalo dung: Effect of $Fe_3O_4$ nanoparticles on methane yield. *Renewable Energy, 133*, 1046-1054. https://doi.org/10.1016/j.renene.2018.10.113

31. Pardilhó, S., Pires, J. C., Boaventura, R., Almeida, M., & Dias, J. M. (2022). Biogas production

from residual marine macroalgae biomass: Kinetic modeling approach. *Bioresource Technology, 359*, 127473. https://doi.org/10.1016/j.biortech.2022.127473

32. Raposo, F., De la Rubia, M., Fernández-Cegrí, V., & Borja, R. (2012). Anaerobic digestion of solid organic substrates in batch mode: an overview relating to methane yields and experimental procedures. *Renewable and Sustainable Energy Reviews, 16*(1), 861-877. https://doi.org/10.1016/j.rser.2011.09.008

33. Rosato, M. A. (2017). *Managing biogas plants: A practical guide*. CRC Press.

34. Schmidt, T., Nelles, M., Scholwin, F., & Proter, J. (2014). Trace element supplementation in the biogas production from wheat stillage– optimization of metal dosing. *Bioresource Technology, 168*, 80-85. https://doi.org/10.1016/j.biortech.2014.02.124

35. Stoddard, I. (2010). Communal polyethylene biogas systems: Experiences from on-farm research in rural West Java.

36. Torres-Lozada, P., Díaz-Granados, J. S., & Parra-Orobio, B. A. (2015). Effects of the incorporation of drinking water sludge on the anaerobic digestion of domestic wastewater sludge for methane production. *Water Science and Technology, 72*(6), 1016-1021. https://doi.org/10.2166/wst.2015.291

37. Wang, M., Tang, S. X., & Tan, Z. L. (2011). Modeling in vitro gas production kinetics: derivation of logistic–exponential (LE) equations and comparison of models. *Animal Feed Science and Technology, 165*(3-4), 137-150. https://doi.org/10.1016/j.anifeedsci.2010.09.016

38. Wang, K., Yun, S., Xing, T., Li, B., Abbas, Y., & Liu, X. (2021). Binary and ternary trace elements to enhance anaerobic digestion of cattle manure: Focusing on kinetic models for biogas production and digestate utilization. *Bioresource Technology, 323*, 124571. https://doi.org/10.1016/j.biortech.2020.124571

39. Wellinger, A., Murphy, J. D., & Baxter, D. (2013). *The biogas handbook: science, production and applications*. Elsevier.

40. Zareei, S. (2018). Evaluation of biogas potential from livestock manures and rural wastes using GIS in Iran. *Renewable Energy, 118*, 351-356. https://doi.org/10.1016/j.renene.2017.11.026

41. Zhang, Y., Feng, Y., Yu, Q., Xu, Z., & Quan, X. (2014). Enhanced high-solids anaerobic digestion of waste activated sludge by the addition of scrap iron. *Bioresource Technology, 159*, 297-304. https://doi.org/10.1016/j.biortech.2014.02.114

42. Zhao, Z., Li, Y., Quan, X., & Zhang, Y. (2017). Towards engineering application: Potential mechanism for enhancing anaerobic digestion of complex organic waste with different types of conductive materials. *Water Research, 115*, 266-277. https://doi.org/10.1016/j.watres.2017.02.067

# بررسی کارایی افزودنی‌های بر پایه آهن در هضم بی‌هوازی کودهای دامی: مطالعه مدل‌سازی سینتیک

جواد رضائی فر[1]، عباس روحانی[1]*، محمدعلی ابراهیمی نیک[1]

**چکیده**

در تلاش برای بهبود عملکرد و پایداری هضم بی‌هوازی (AD)، افزودنی‌های مبتنی بر آهن به‌عنوان ریزمغذی‌ها و لجن تصفیه آب آشامیدنی (DWTS) می‌توانند نقش کلیدی داشته باشند. این مطالعه به بررسی سینتیک تولید متان در طول AD کودهای گاوی می‌پردازد که شامل غلظت‌های مختلف Fe و $Fe_3O_4$ (۱۰، ۲۰ و ۳۰ میلی‌گرم در لیتر) و DWTS (۶، ۱۲ و ۱۸ میلی‌گرم در لیتر) می‌شود. با استفاده از یک کتابخانه گسترده از مدل‌های رگرسیون غیرخطی (NLR)، ۲۶ نامزد مورد بررسی قرار گرفتند و هشت مورد به‌عنوان پیش‌بینی‌کننده‌های قوی برای کل فرآیند تولید متان ظاهر شدند. مدل Michaelis-Menten به‌عنوان انتخاب برتر برجسته شد و سینتیک کودهای دامی AD را با افزودنی‌های مشخص‌شده آشکار کرد. یافته‌ها نشان داد که سطوح مختلف DWTS بالاترین تولید متان را به‌همراه دارد، در حالی‌که $Fe_3O_420$ و $Fe_3O_430$ کمترین میزان را ثبت کردند. قابل‌ذکر است، DWTS6 تولید متان تقریباً ۳۴٪ و ۴۲٪ را در مقایسه با Fe20 و $Fe_3O_430$ نشان داد و آن را به‌عنوان موثرترین تیمار معرفی کرد. علاوه بر این، DWTS12 بالاترین میزان تولید متان را به نمایش گذاشت و به ۱۴۷/۶ سی‌سی در روز ششم رسید. با تأکید بر مفاهیم عملی، این تحقیق بر کاربرد مدل پیشنهادی برای تجزیه و تحلیل سایر پارامترها و بهینه‌سازی عملکرد AD تأکید می‌کند. این مطالعه با بررسی پتانسیل افزودنی‌های مبتنی بر آهن و DWTS، مسیر را در تولید متان از کودهای گاوی و پیشبرد شیوه‌های مدیریت زباله پایدار هموار می‌سازد.

**واژه‌های کلیدی:** عناصر کمیاب، کود دامی، مدل‌سازی، مطالعه سینتیک، هضم بی‌هوازی

---

۱- گروه مهندسی بیوسیستم، دانشکده کشاورزی، دانشگاه فردوسی مشهد، مشهد، ایران

(*- نویسنده مسئول: Email: arohani@um.ac.ir)